FORMULATION AND EVALUATION OF MOUTH-DISSOLVING ORAL FILM OF NICOTINE USING QUALITY BY DESIGN APPROACH

SACHIN DATTRAM PAWAR[1,2] ID, NAGOJI SHINDE[2], GUNDAWAR RAVI[1] ID, TUKARAM KALYANKAR[2*] ID

[1]Department of Pharmaceutical Quality Assurance, Manipal College of Pharmaceutical Sciences, Manipal Academy of Higher Education, Manipal, India. [2]Department of Quality Assurance, School of Pharmacy, Swami Ramanand Teerth Marathwada University, Vishnupuri, Nanded-431606, Maharashtra, India
*Corresponding author: Tukaram Kalyankar; *Email: kalyankarr@gmail.com

ABSTRACT

Objective: Nicotine is a natural alkaloid found in *Nicotiana tabacum* and is widely used as a potent stimulant. This study aims to extract and characterize nicotine from tobacco powder and formulate a nicotine-containing Oral Fast-Dissolving Film (OFDF) for nicotine replacement therapy.

Methods: Nicotine was extracted from tobacco using water and Hydrochloric Acid (HCL). Purification was performed using column chromatography. The extracted nicotine was characterized using UV-visible spectroscopy, XRD, SEM, and FTIR. The OFDF was prepared using a Quality by Design (QbD) approach; a factorial design 3x3 was employed for film optimization. The solvent casting method was used for film preparation. The optimized formulation was evaluated for folding endurance, disintegration time, and drug release. Stability studies were performed as per ICH guidelines.

Results: The extraction process successfully yielded purified nicotine in crystalline form, having a crystalline index of 88.89%. The extracted nicotine shows lambda max at 260 nm; the FTIR study confirms the stretching and bending vibration frequencies for nicotine. The polymer Hydroxypropyl Methylcellulose (HPMC-E5) and plasticizer Polyethylene Glycol (PEG) concentrations (w/w) were selected as independent variables. At the same time, disintegration time, folding endurance, and dissolution time were evaluated as dependent variables for QbD. All the formulations were assessed, and FF3 is the optimized batch based on the dissolution, drug content, and folding endurance.

Conclusion: Nicotine was extracted and purified. The purified nicotine was then incorporated into an OFDF, which exhibited rapid disintegration and dissolution. This formulation can aid patients experiencing nicotine withdrawal symptoms by providing a safer, immediate nicotine release.

Keywords: Nicotine, Extraction, OFDF, Powder characterization, SEM, XRD

INTRODUCTION

Oral Fast-Dissolving Film (OFDF) has recently gained popularity in the pharmaceutical industry because of its immediate release action. This OFDF was developed based on the transdermal patch technology OFDF [1]. OFDF disintegrates within a minute when it comes in contact with the saliva and releases the drug [2]. The OFDF system emerged as an economical way of administering unit doses of medication to normal, pediatric, and geriatric patients who have difficulty swallowing standard pills, capsules, liquid orals, or syrup [3]. The delivery method comprises a thin oral strip that quickly absorbs saliva, hydrates rapidly, and sticks to the application site [4] when placed under the patient's tongue [5]. The film then disintegrates and dissolves, releasing the drug for absorption through the mucosal route. This maintains quick-dissolving properties and allows gastric absorption when ingested [6].

Recently, research has focused more on the buccal and sublingual drug delivery systems because of their unique anatomy and physiology. Nicotine pouches recently caught researchers' attention. It is a new class of nicotine products and is non-intrusive and appealing, especially to younger demographics [7]. Some studies raise concerns about the safety of nicotine pouches used in the US for smoking cessation, prompting researchers to analyze their trends [8]. Researchers are also working on the potential of oral film alternatives to conventional tablets for erectile dysfunction treatment. A novel sildenafil citrate-loaded orally dissolving film was prepared for rapid disintegration [9]. The combination of dexamethasone oral film was provided to the breast cancer patient undergoing highly emetogenic chemotherapy as an antiemetic [10].

The Quality by Design (QbD) principle has led to significant advancements in drug delivery, especially in formulation optimization [11]. The preparation and characterization of solid lipid nanoparticles for bioavailability enhancement follow a QbD approach to ensure quality and performance [12]. The systematic use of QbD helps to improve product quality consistency, optimize formulation process parameters, regulatory compliance, faster approval, and cost-time efficiency in development [13, 14].

Nicotine is an exogenous agonist for most nicotinic acetylcholine receptors (nAChRs), except nAChRα9 and nAChR10 [15, 16]. Found in *N. tabacum, D. hopwoodii, A. syriaca,* and *N. rustica* leaves (2–14%), its delivery remains challenging due to physicochemical properties and adverse effects. Nicotine is highly addictive [17].

Nicotine is one of the most commonly abused substances. It acts as a Central Nervous System (CNS) stimulant. An ordinary cigarette delivers 1–2 mg of nicotine, while excessive doses (30–60 mg) can be hazardous. In animals, it induces both anxiety and behavioral excitement [18]. Nicotine addiction involves drug-reinforced behavior, compulsive use, and relapse after withdrawal. It includes tolerance, sensitization, and both physical and psychological dependence. Withdrawal symptoms include distress, depressed mood, tension, anxiety, irritability, difficulty concentrating, and sleep disturbances [19]. According to the survey, nicotine is the most addictive drug. Quitting smoking is complex and may need multiple efforts; people who stop smoking frequently relapse due to withdrawal symptoms, stress, and weight gain [20, 21]. Tobacco smoke contains a lethal combination of over 7,000 compounds, of which hundreds are toxic and approximately 70 can cause cancer. Smoking raises the chance of significant health problems, a variety of diseases, and even death. People who cease smoking have a much lower risk of disease and premature mortality. However, the health benefits to people are more significant [22].

Many nicotine delivery systems are available on the market, such as nicotine gums, lozenges, nicotine pouches, and ENDS (electronic nicotine delivery systems). In the case of nicotine chewing gum, active chewing is required, and an older person cannot chew for a

long time. As mentioned above, nicotine pouches have raised regulatory concerns [23, 24]. Nicotine film is appropriate for smokers who take their first cigarette of the day more than 30 min after awakening. On the tongue, place one film. To dissolve the nicotine film, close the mouth and gently press the tongue on the roof of the mouth for around three minutes. By reducing the frequencies, people can quit the habit of nicotine consumption [25].

This study aims to develop nicotine-containing OFDF using excipients like Hydroxypropyl methylcellulose (HPMC) Premium E5 lV, polyethylene glycol, citric acid, Tween 80, saccharin, and menthol to enhance patient acceptability. Nicotine was extracted from raw tobacco and characterized using Scanning Electron Microscopy (SEM), Powder X-ray Diffraction (PXRD), Differential Scanning Calorimetry (DSC), and Fourier Transform Infrared Spectroscopy (FTIR). The film was prepared using the solvent casting method and a simple factorial design based on the QbD approach. Key parameters such as disintegration time, tensile strength, and folding endurance were evaluated.

MATERIALS AND METHODS

Material

The analytical and laboratory-grade excipients supplied by the different vendors' nicotine were obtained from Sigma Aldrich. HPMC-E5 was procured from Colorcon Asia Pvt. Ltd., India, Tween 80 from Merk India Pvt. Ltd., glycerine from Sumer Company, and PEG 400 from Qualigens Fine Chemicals. The tobacco power was purchased from the nearby Sai pan shop in Vishnupuri, Nanded. Sigma-Aldrich India Pvt. Ltd. provided the solvents and other chemicals. The Department of Pharmaceutical Quality Assurance installed a MilliQ water system that used water for formulation and other activities.

Methods

Extraction of nicotine from tobacco

Different extraction methods were tried to isolate crystalline nicotine from tobacco, mainly water, water and lemon juice, and nicotine extraction using NaOH and petroleum ether [26, 27]. Nicotine extraction uses HCL, benzene, and water, and extraction uses water and HCL acid. The different extraction methods were assessed to isolate pure nicotine, and we finalized the technique depending on the % recovery. The extract powder was dissolved in water, and the UV-visible spectroscopic analysis was performed to check the maximum lambda [28]. The purity study was conducted using UV-visible spectroscopy. Nicotine extraction using water and acid was done for the final extraction, depending on the recovery percentage. The procedure followed was to mix 1 g of tobacco with 10 ml of water and add hydrochloric acid until the blue litmus paper turned red. This addition is because nicotine is a weak base, and at low pH, it will form water-soluble salt nicotine HCL, increasing aqueous solubility. This solution is covered and placed for 24 h [29]. After the 24 h filter, the mixture is filtered using filter paper. The residue is removed, the filtrate is collected, and the solution is heated under a burner. The water molecules will evaporate, and the nicotine extract will be concentrated at the bottom of the beaker; a black nicotine powder will be observed. Purification of extracted nicotine was performed using column chromatography, as reported. The stationary phase was prepared by dissolving 70 g of silica gel 60 in 250 ml of petroleum ether, with an ethanol ratio of 80:20. The extracted 2 gm of black powder was mixed with 2 gm of silica gel powder and dried for 15 min, gently loaded on the silica bed, and run through the chromatography. 250 ml of PE: Ethanol (80:20) is used as the mobile phase, and the stopcock is opened to maintain continuous solvent flow to prevent dryness. Collect the fraction and check for the UV to confirm the lambda max. After all the fractions are subjected to the rota evaporator, a yellow crystal of nicotine is collected and stored in the freezer for further characterization [30].

Characterization of extracted nicotine powder

Physical appearance and solubility

The nicotine extract was visually checked for color, odor, and appearance; the solubility of the nicotine extract was checked in different solvents like water, ethanol, and methanol [31, 32].

Ultraviolet-visible spectroscopy

The Shimadzu UV-1800 UV-visible spectrophotometer was used to analyze the extracted nicotine's lambda max, assess purity, and quantify it. It was used for other studies, such as dissolution and content uniformity of the OFDF film. The stock solution (1000 ug/ml) was prepared by dissolving 1 mg of nicotine in 1 ml of water, from which further serial dilutions were prepared and used for the analysis. Prepared a standard 100 ug/ml solution by diluting stock solution and scanned it in the 200-800 nm range to determine λ max. The calibration curve was prepared for purity analysis and quantification [33]. Purity analysis was performed by comparing with standard absorbance calibration curves prepared to measure the absorbance at λmax and plot Absorbance vs. Concentration, followed by an analysis of the sample and comparison of expected vs. observed concentration to estimate purity [34].

FTIR

An FTIR spectroscopy was conducted on the extracted nicotine powder used in the drug excipient compatibility study. The process consisted of putting a nicotine sample in an FTIR Sample holder. The nicotine sample was placed in the light path and scanned over the wavenumber 4000-400 cm^{-1} range on Shimadzu FTIR Prestige-21. The obtained spectrum was recorded. For drug excipient compatibility, the second sample was a physical mixture of nicotine extract with an excipient sample, weighted and scanned over the 4000-400 cm^{-1} range. The obtained spectrum was recorded [35].

SEM

SEM studies were performed to check the surface morphology of the extracted powder. The samples were analyzed using the JEOL JSM-6390LV made by JEOL Limited, Tokyo (Japan). The sample was placed in a sample holder, and at ×1000 magnification, images were captured from different angles using a tungsten filament as the electron source. The surface morphology of the extracted nicotine powder was analyzed using SEM at various magnifications (2.00 KX and 10.00 KX) [36, 37].

PXRD

The diffraction pattern for nicotine extracting powder was recorded using Goniometer Ultima4, model generator (S. R. T. M. U. Nanded University, Nanded) in the 10°-80° 2-theta scale with k-″ß filter. The position and intensities of diffraction peaks were considered, and the crystalline of the drug was compared [38, 39].

Formulation of the nicotine-containing film

Drug-excipient compatibility study

The Drug-excipient compatibility study was performed to understand the nicotine compatibility with the HPMC E5. The physical mixture of extracted nicotine and HPMC E5 was prepared in a commonly used 1:1 ratio and thoroughly mixed using a mortar and pestle. The KBr pellet method was used to prepare the sample. FTIR samples were prepared by mixing 1 mg of the sample with 100 mg of dry KBr, grinding to a fine powder, and pressing into a thin, transparent pellet. Analyze the prepared physical mixtures using FT-IR and record the spectra. Data was analyzed by focusing on the functional group present in the nicotine molecule [40].

Formulation and development of OFDF

The solvent casting method was used for the OFDF preparation. A simple factorial design (quality-by-design) approach was used for formula optimization, with Design-Expert software (Stat-Ease) for analysis. The parameters like Quality Target Product Profile (QTPP), Critical Quality Attributes (CQA), and critical process parameters were defined, and independent and dependent variables were selected [41, 42]. The table for this is mentioned in the supplementary files. In independent variables, the concentration of polymer (w/w) and plasticizers (w/w) were selected while the dependent disintegration time, folding endurance, and dissolution time were set. Please check tables T1 and T2. A simple solvent casting method was used, where the film was formed using a polymer and plasticizer ratio in a tiny beaker.

In this method, the water-soluble polymers are first dissolved at 1,000 rpm and heated to 40 °C. All other excipients, such as colors, flavoring

agents, and sweetening agents, are dissolved separately. Both solutions are then mixed thoroughly while stirring at 1,000 rpm. The resulting solution is then combined with nicotine dissolved in water. Entrapped air is removed using a vacuum. The final solution is cast into a film and allowed to dry before being cut into pieces of the desired size. The target thickness range was set at 100–200 μm and ensured using a micrometer screw gauge. After casting, the film is placed in an oven at 40 °C for drying for 4 h. Once dried, it is stored in a desiccator to prevent moisture absorption. HPMC E5 lV was selected as the polymer at a 1–3% concentration due to its low viscosity, which enhances the film's hydration and swelling. It is widely used in preparing mouth-dissolving films and is classified as GRAS (generally recognized as safe) and biocompatible. The concentration range was chosen to optimize film properties, ensuring adequate flexibility and mechanical strength. PEG was used as a plasticizer within a 0.5–1.5% range. PEG is commonly used as a plasticizer to improve film flexibility and reduce brittleness while enhancing drug release.

Additionally, HPMC and PEG are compatible, and the selected concentration range (0.5–1.5% w/w) maintains a balance between mechanical strength, flexibility, and drug release. Similarly, nicotine extracted power was dissolved in another beaker in a 2 mg dose, and both phases were mixed on the magnetic stirrer for 30 min. It mixes appropriately, and then it casts on the Petri dish. After completely drying, cut the film to the required size [43-45].

Dose calculation

The calculation of the dose and diameter of the film can be changed if we fix the diameter to 2.5*2 cm. The total 16 films can be formulated in one Petri dish with a dose of 2 mg using the calculation as mentioned below

Amount of drug present in one film = 2 mg

Diameter of proposed film =2.5*2 cm

Area of the film = 5 cm^2

The diameter of the plate = 8.8 cm

Radius of the plate = 8.8/2 = 4.4 cm

Area of the plate = πr^2 = 3.14*(4.4)^2

=3.14*19.36

=60.86 cm^2

Number of films present in the proposed area of the plate = area of plate/area of the film

= 60.86/5

= 12.17

Table 1: Independent variables in the design experts

Factor	Level used, actual (coded)		
Independent variables	Low (_1)	Medium (0)	High (+1)
X1= concentration of polymer (% w/w)	1	2	3
X2= concentration of plasticizer (% w/w)	0.5	1	1.5

Table 2: Batch optimization formula generated by design experts

S. No.	Film formula	Polymer (mg)	Plasticizer (mg)	Saliva stimulating agent (mg)	Sweeting agent (mg)	Drug (mg)
1	FF1	100	50	50	50	30
2	FF2	200	100	50	50	30
3	FF3	300	150	50	50	30
4	FF4	100	100	50	50	30
5	FF5	200	50	50	50	30
6	FF6	200	150	50	50	30
7	FF7	300	100	50	50	30
8	FF8	300	50	50	50	30
9	FF9	100	150	50	50	30

Evaluation of OFDF

Film thickness

The thickness of the film is calculated by using a micrometer screw gauge. The film thickness was measured at five positions, i.e., the center and the four corners, and the mean thickness was calculated. This test was performed on three films of each formulation. The maximum variation in the thickness of the films should be less than 5%, and the mean±SD should be calculated.

Film transparency

Film transparency is tested with an open eye. The film was placed on a black background, patterns that appeared throughout the film were observed, and clarity, i.e., transparency, was checked.

Weight variation

For the weight variation test, the film's mean weight was recorded. The standard deviations of weight fluctuation were calculated using the mean value.

Folding endurance

The folding endurance value calculates how often the film can be folded without breaking. The numbers of folds were calculated.

In vitro drug release study

The study uses 50 ml of phosphate buffer with pH 6.8 maintained; the temperature was set at 37±0.5 °C and stirred at 50 rpm. The sample was withdrawn at predetermined intervals of 2 and 4, 6, 8, and 12 min. The fresh media was withdrawn and replaced with one ml to maintain the sink condition of the drug analyzed using UV-visible spectroscopy [46].

Disintegration test

The petri dish method was used to check the disintegration time of the oral film. 1 ml of distilled water was placed in a Petri dish, and one film was added to the water's surface. The time was measured until the oral film was dissolved entirely [46].

Stability study of OFDF

Stability is an essential part of any formulation; this stability study has been performed by following the guidelines of the International Conference on Harmonization (ICH). The optimized formulation was developed and packaged in a specific way. It was wrapped in aluminum foil after first wrapping it in butter paper, and then it was put in an aluminum pouch and sealed with heat. The acceptable storage temperatures for formulations are 30 °C/60% RH and 40 °C/75% RH. After a month, the films were evaluated for drug content, disintegration time, and physical look [47].

RESULTS AND DISCUSSION

Extraction and purification of nicotine from tobacco

Fig. 1 shows the extraction of nicotine and column chromatography for the purification technique. The extraction of nicotine is a crucial

aspect of this study since we require nicotine, but it must be highly pure to prepare the film. Different extraction methods were tried, which are listed in the methodology section. One of the extraction techniques, NaOH and petroleum ether, found nicotine picrate salt. However, this compound is unsafe for consumption due to its toxicity. So instead, we tried other acids like tartaric and citric acid, but no positive result was found. Fig. S1 in the supplementary files provides images of the different acids used. The three methods,

nicotine extraction using NaOH, petroleum ether, and nicotine extraction using HCL, benzene, and water, and extraction using water and acid, were shown to have the lambda max of nicotine. The % yield of these three methods was nicotine picrate, 0.1%; extraction using benzene, 0.5%; and extraction using water and acid, the highest 1.8% yield. The extraction using water and acid was further purified using column chromatography. After collecting all the aliquots, a rota evaporator evaporated the solvent.

Fig. 1: Purification of the extracted nicotine using column chromatography

Characterization of extracted nicotine powder

Physical appearance and solubility

The extracted nicotine powder is a yellowish, odorless crystalline substance. Solubility studies indicate it is moderately soluble in water, freely soluble in ethanol, and insoluble in chloroform.

UV-visible scanning spectrophotometer

The 20 μg/ml of a nicotine solution was scanned from 200 to 400 nm wavelength, showing maximum absorbance at 260 nm, which complies with the reported value [48]. Fig. 2 shows the UV spectra of nicotine and the standard calibration curves. The calibration curve of pure nicotine was prepared to quantify the nicotine from the extracted formulation. The calibration curve for UV analysis showed a linear relationship with the equation Y = 0.006x+0.026y and a high correlation coefficient (R^2 = 0.996), indicating excellent linearity. The limit of detection (LOD) and quantification (LOQ) using LOD=3.3×SD/slope and LOQ=10×SD/slope standard deviation is 0.02. The LOD = 1.10 μg/ml and LOQ = 3.33 μg/ml, respectively.

The same calibration curve was used for the quantification of extracted nicotine.

FTIR

The FTIR study was performed on extracted nicotine powder to confirm the stretching and bending vibrations in the extracted powder. The study found similar stretching and bending for extracted nicotine compared with pure nicotine. C-H bending and stretching for extracted nicotine is 904 and 2970, while pure nicotine is 904 and 2780 cm^{-1}. Similarly, C=C and C=N stretching for extracted nicotine is 1667 and 1712 cm^{-1}. Table 3 shows the stretching and bending vibrations found in the FTIR spectra.

In comparison, pure nicotine is 1644 and 1691 cm^{-1}, respectively. The FTIR study confirms similar stretching and bending vibrations. FTIR spectra of extracted nicotine are shown in fig. 3.

SEM

SEM image reveals the crystalline structures with diverse shapes and particle sizes. Particles appear angular, faceted, suggesting the crystalline nature of the extract. Some aggregation has been found, which may be due to the drying process of the extraction. The image also explains that the particles are uniform in size. Crystalline particles exhibit smooth surfaces with minimal irregularities, confirming the absence of impurities or amorphous regions in the extracted nicotine. The SEM image of extracted nicotine is shown in fig. 4 [49]**.**
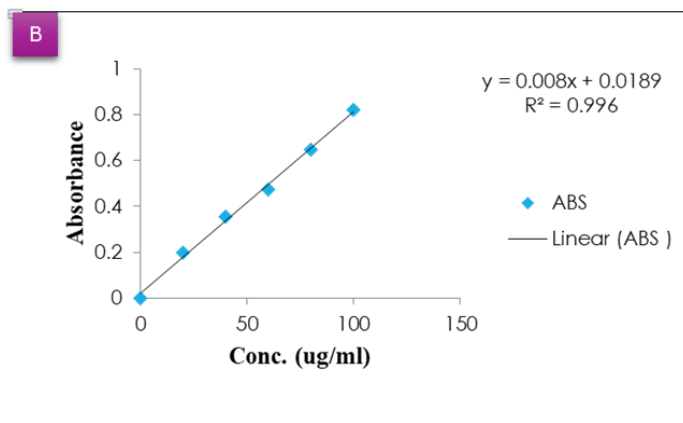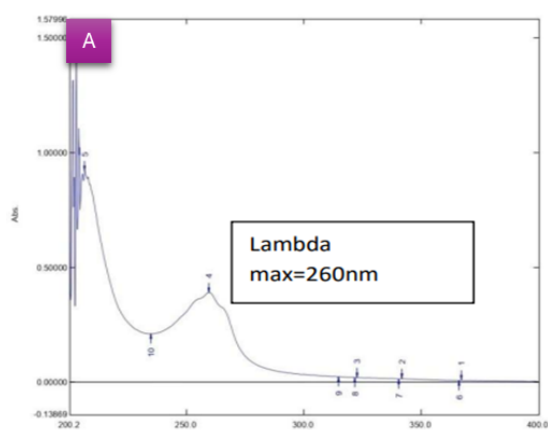

Fig. 2: UV-visible spectra of A) extracted nicotine powder, B) Calibration curve graph
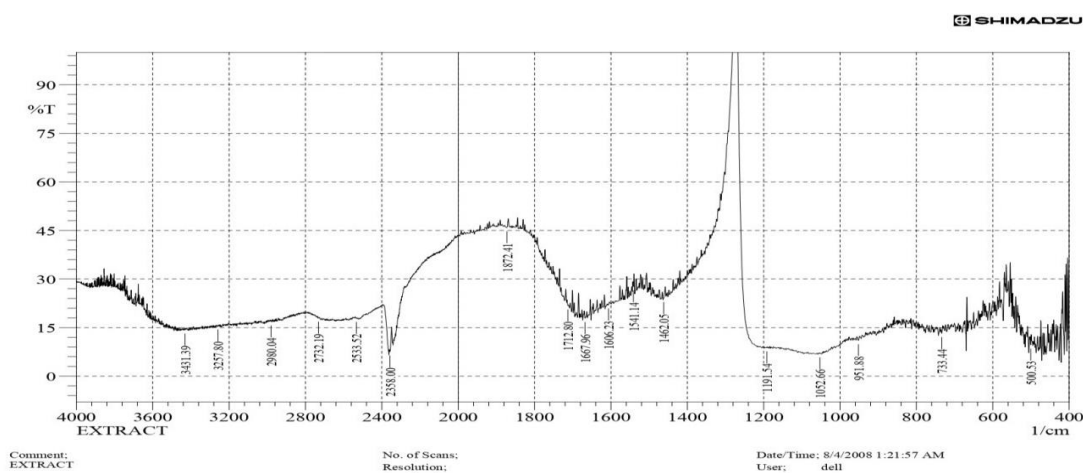
Fig. 3: FTIR spectra of extracted nicotine

Table 3: Stretching and bending vibration of pure nicotine and extracted nicotine

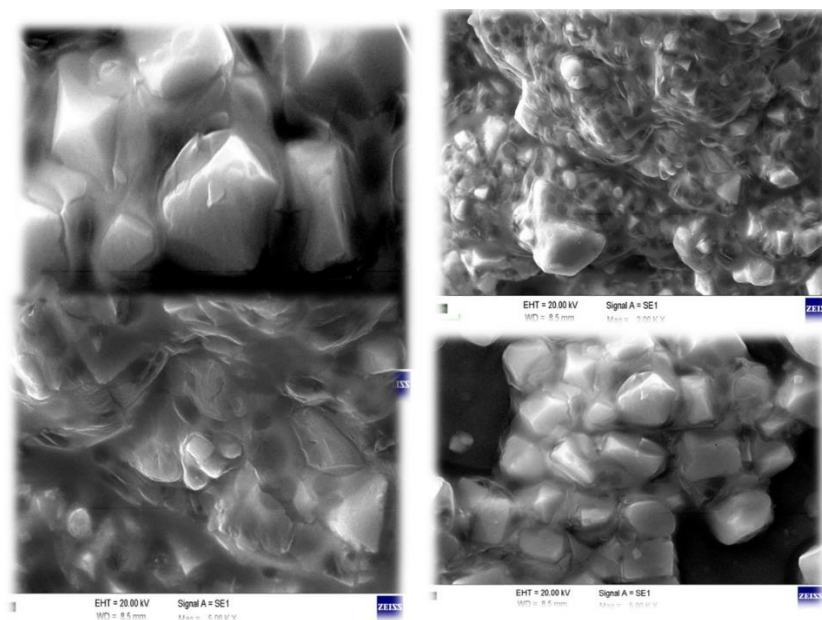| Stretching/Bending	Pure nicotine	Extracted nicotine
C-H bending	714, 904	733,951
C=N	1644	1667
C=C	1691	1712
C-H Stretching	2970-2780	2980-2780

Fig. 4: SEM image of extracted nicotine powder

PXRD

The PXRD study of extracted nicotine suggests that most of the 2θ values match with the pure nicotine diffraction pattern for pure crystalline nicotine, which is typically observed around 2θ = 10°, 17°, 20°, 25°, and 30°. If compared with the extract, the ~31° peak in the extract closely aligns with a significant peak reported for pure nicotine (~30°), indicating the presence of crystalline nicotine. The other peaks, such as ~12° and ~44°, may be due to degradation or other forms of crystals. The PXRD spectra are shown in fig. 5. The crystallinity index was calculated using a simple, widely used Segal method—intensity values at specific angles (2θ). The highest and minimum intensities were fitted into the formula and calculated per this method, indicating a high degree of crystallinity in the sample; nicotine exhibits significant crystalline characteristics [50, 51].

$$\text{Crystallinity Index CI} = \frac{I002 - Iam}{I002} X100$$

Where:

I002 = Intensity of the strongest crystalline peak

Iam = Intensity of the amorphous background (typically the lowest intensity value between crystalline peaks)

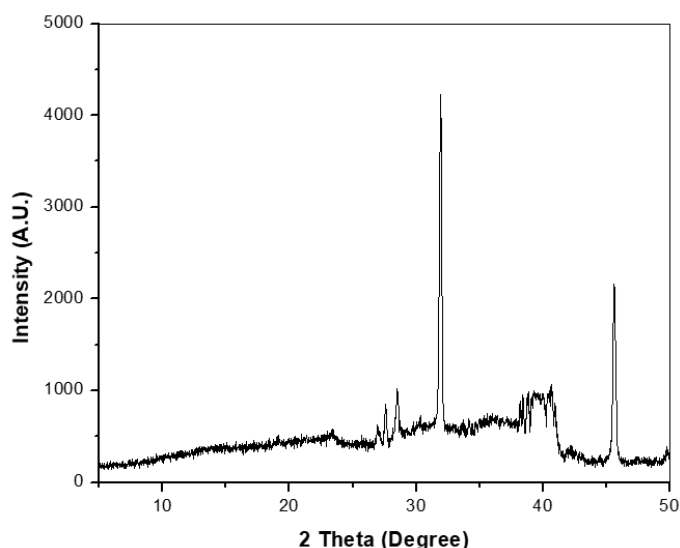$$CI = \frac{4500 \text{ A. U.} - 500 \text{ A. U.}}{4500 \text{ A. U.}} X100$$

$$CI = 88.89\%.$$

Fig. 5: XRD spectra of extracted nicotine powder

Formulation of the nicotine-containing OFDF

Drug-excipient compatibility study

The drug-excipient compatibility study was performed using FTIR spectroscopy. Samples were analyzed to examine the bending and stretching vibrations of nicotine. In the mixture, nicotine-bending frequencies C-H, C=N, and C=C bend at 714, 1644, and 1691, respectively. Similarly, stretching frequencies for C-H show 2908, confirming that the nicotine extract is compatible with the excipients, as shown in fig. 6. Nicotine is a volatile and hygroscopic alkaloid that may undergo oxidation in the presence of oxygen. Film-forming excipients like HPMC can help minimize nicotine loss. The interaction of HPMC with nicotine through hydrogen bonding can influence drug release [50].
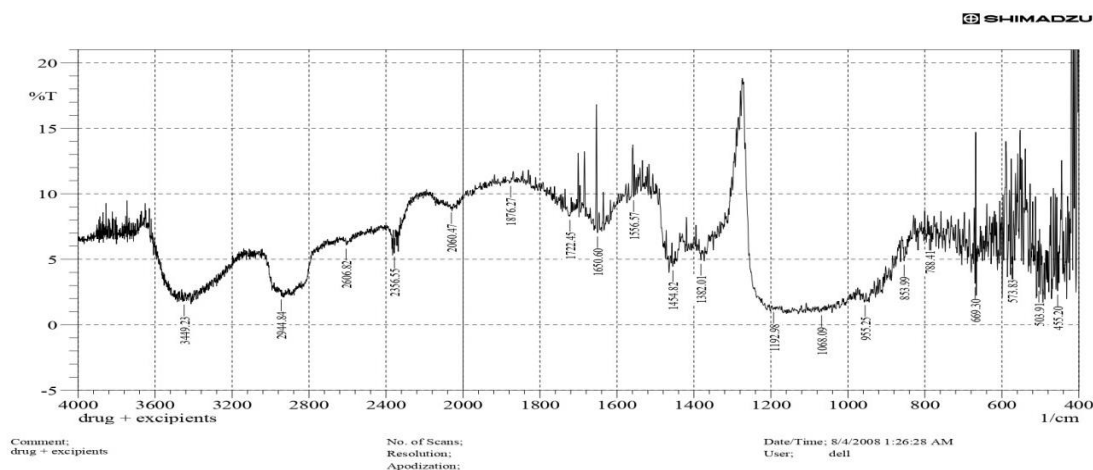

Fig. 6: FTIR spectra of extracted nicotine with HPMC

Table 4: Result of all batches design expert

Run	Batch	Independent Variables		Dependent variables		
		X1	X2	Y1	Y2	Y3
1	FF1	-1	-1	95.6900±0.8627	14±1	12.66±2.51
2	FF2	0	0	92.9500±1.1879	14±1	16.66±2.08
3	FF3	1	1	96.0550±0.2192	17±1.52	18.33±3.51
4	FF4	-1	0	95.8400±1.1314	11±1	30.66±3.05
5	FF5	0	-1	92.5550±1.6193	16±1.73	6.0±2
6	FF6	0	1	95.9300±0.5233	13±3	27±3
7	FF7	1	0	91.9550±2.6092	19±1	8.0±3
8	FF8	1	-1	91.2450±2.3405	22±1.73	3.0±1
9	FF9	-1	1	97.7900±0.5515	09±1	51.33±4.04

X1= Concentration of polymer (% w/w); X2 =concentration of plasticizer (% w/w); Y1 =drug release (%); Y2 = disintegration time (s); Data is given in mean±SD (n=3)

Formulation and development

For optimization, the placebo film was prepared using the solvent casting method. Further, the nicotine film preparation formula was optimized by applying different concentrations to the Design Expert software. The nine different batches of the film were prepared and evaluated, including drug release, disintegration time, and folding endurance. The statistical method Analysis of Variance (ANOVA) test was applied to check the p-value, model F value, and significance. The p-value and F value are Design Expert output, which suggests that this model is highly significant. The FF3 was the final formula selected for further studies on stability

and other evaluations. Table 4 shows the detailed results of optimized experiments. Table 5 shows the statistical significance (ANOVA results) for % drug release, disintegration time, and folding endurance. The extracted powder was used to prepare the film, but it was found to be improperly formulated before column chromatography. However, the film was formed after purification, as shown in fig. 7. The three different films are shown in the figure. First, the extracted powder of nicotine picrate was where the yellow film was observed; second, the extraction method of water and acid is a net-like film observed before column chromatography; and the final film was extracted, purified by column chromatography material, and used.
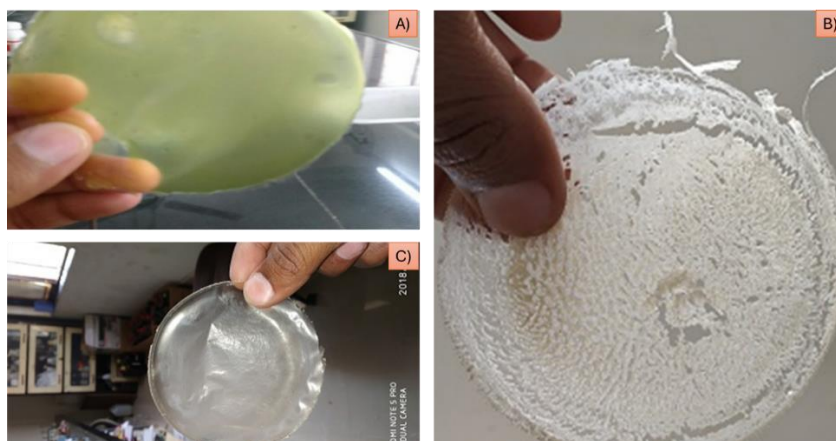

Fig. 7: A) Film prepared using nicotine picrate crystals B) Film prepared before column chromatography C) Film prepared after column chromatography.

Fig. 8 shows (a) a counterplot of drug release (Y1) (b): The curved surface shows a clear interaction between polymer and plasticizer concentrations on drug release. The curved surface shows how the amounts of plasticizer and polymer affect drug release. Drug release increases when polymer content is low and plasticizer concentration is high (red zone). The surface progressively slopes downward as the polymer concentration rises, demonstrating the inhibitory effect on drug release. Drug release is higher (red region) when polymer concentration is low and plasticizer concentration is high. The surface

gradually slopes downward as polymer concentration increases, confirming its inhibitory effect on drug release. 3D response surface plot of drug release (Y1) shows the polymer and plasticizer effect. Higher polymer concentrations decrease drug release, most likely due to slower drug diffusion across the polymer network or an increased matrix density. Higher drug release is made possible by the matrix's decreased density at lower polymer concentrations. Drug mobility is improved by increasing the concentration of the plasticizer, which also reduces the stiffness of the polymer matrix.
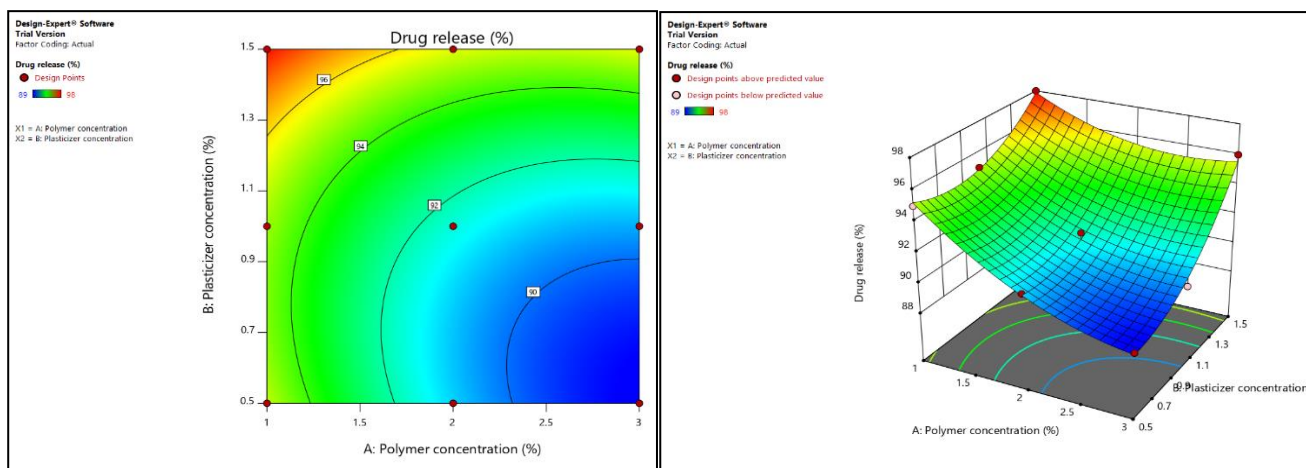

Fig. 8: (a) a counterplot of drug release (Y1) (b): The curved surface shows a clear interaction between polymer and plasticizer concentrations on drug release left image (Contour plot) (High drug release) → Green → Blue (Low Drug Release). Right image (3D Surface Plot) color gradient: yellow (High drug release) → Green → Blue (Low drug release)

In fig. 9(a), a Counter plot of disintegration time (Y2) (b): 3D response surface plot for disintegration time (Y2). Low Disintegration Time (Blue Region): At high plasticizer and low

polymer concentrations. A high disintegration time (red region) was noted at high polymer and low plasticizer concentrations. As plasticizer content falls and polymer concentration rises, the

disintegration time lengthens. The relationship between polymer and plasticizer concentrations is visually understood thanks to the

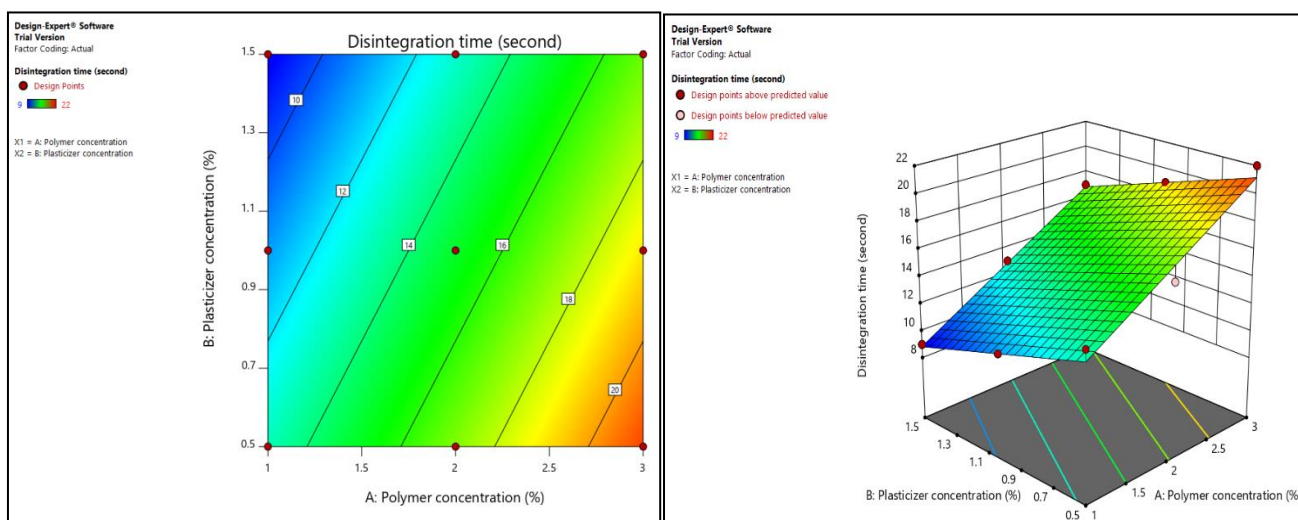3D figure, which shows how the disintegration time varies depending on the two parameters.

Fig. 9: (a), a Counter plot of disintegration time (Y2) (b): 3D response surface plot for disintegration time (Y2). Left Image (Contour Plot) Color Gradient: Blue (Low disintegration time) → Green → Yellow (High disintegration time) Right Image (3D surface plot) Color Gradient: Blue (Low disintegration time) → Green → Yellow (High disintegration time)

Fig. 10 (a): Counter plot of folding endurance (Y3) (b): 3D response surface plot of folding endurance (Y3) Folding endurance is highest in regions where both polymer and plasticizer concentrations are balanced. Low polymer

concentration with low plasticizer concentration results in poor folding endurance (blue areas). Optimal folding endurance (yellow to red regions) occurs at moderately high polymer and plasticizer concentrations.
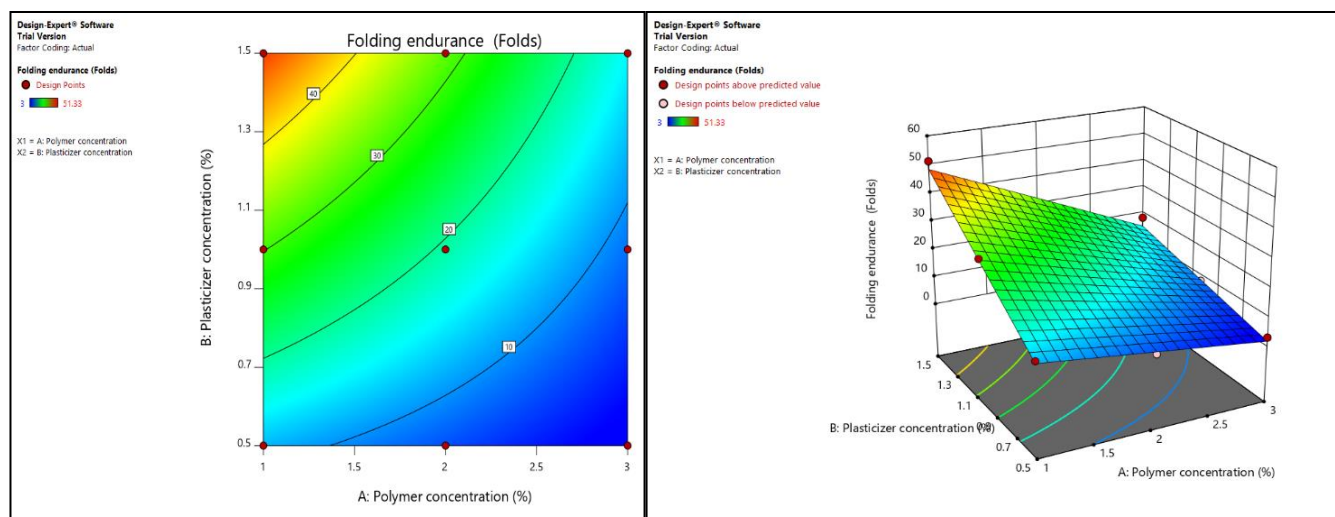

Fig. 10: (a): Counter plot of folding endurance (Y3) (b): 3D response surface plot of folding endurance (Y3) Left Image (Contour Plot) Color Gradient: Blue (Low Folding Endurance) → Green → Yellow (High folding endurance) Right Image (3D surface plot) Color gradient: Blue (Low folding endurance) → Green → Yellow (High folding endurance)

Table 5: Statistical significance (ANOVA results) for % drug release, disintegration time, and folding endurance

Response	Source	Sum of squares	df	Mean square	F-value	P-value	Significance
% Drug release	Model	73.11	5	14.62	39.48	0.0061	Significant
	A-Polymer Concentration	28.17	1	28.17	76.05	0.0032	Significant
	B-Plasticizer concentration	32.67	1	32.67	88.2	0.0026	Significant
Disintegration time (sec)	Model	124.17	2	62.08	97.17	<0.0001	Significant
	A-Polymer concentration	96	1	96	150.26	<0.0001	Significant
	B-Plasticizer concentration	28.17	1	28.17	44.09	0.0006	Significant
Folding endurance (Folds)	Model	1784.81	3	594.94	57.51	0.0003	Significant
	A-Polymer concentration	711.12	1	711.12	68.74	0.0004	Significant
	B-Plasticizer concentration	937.5	1	937.5	90.62	0.0002	Significant

Evaluation of OFDF

The film thickness was measured; the average thickness of the film is 0.065±0.012 mm. All films are transparent when seen visually. The weight variation test was performed individually; the average weight variation of the films was 0.0350±0.0024 g. Folding endurance is calculated by the number of times the film is folded without breaking, which is computed as the folding endurance value. The average folding endurance of the films is approximately 19.29 folds. In an *in vitro* drug release study, within 12 min, 95% of the drug was released from the film, as shown in fig. 11. The obtained data is fitted into various release kinetics models table 6, and the zero-order release kinetics followed by this study show good R^2, high MSC, and low AIC. In all the films, the average disintegration time is less than 30 sec using the petri dish method. The surface pH of the film was 6.68±0.02. It is essential to consider the film's pH since nicotine's stability is pH-dependent in the case of acidic conditions. A pH under six can cause nicotine's protonation, which is helpful for solubility but will hinder absorption in alkaline conditions. A pH of more than 8 can promote oxidation and degradation, forming nicotine N-oxide. Therefore, the maintained pH is close to neutral (6.5-7.5) to ensure nicotine stability [52], [53]. The ideal pH for oral films typically falls within the range of 5.5 to 7.0 for patient comfort, and the saliva pH is usually between 6.2 and 7.6. The detailed evaluation parameters are mentioned in table 7.
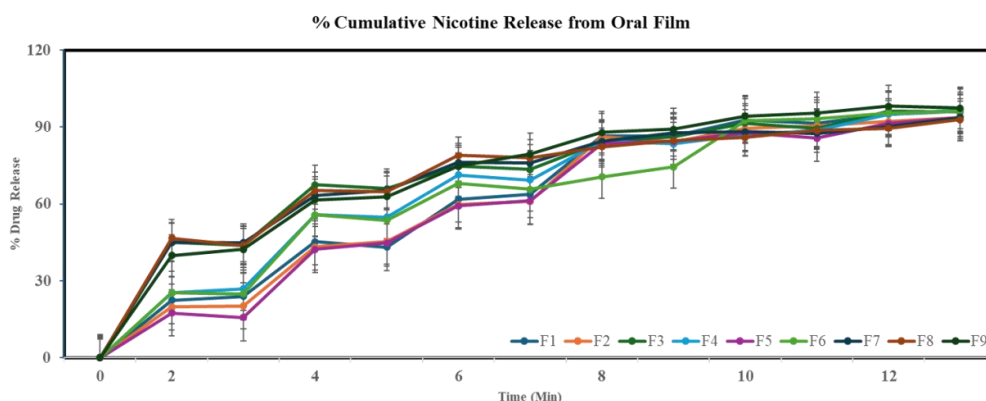

Fig. 11: *In vitro* **drug release study from the oral film, data is given in mean±SD. (n=3)**

Table 6: Nicotine oral film release kinetics

Zero-order	R^2	MSC	AIC
	0.965	48.2722	-0.5814 (Best)
First-order	0.9911 (Second highest)	26.5013	3.0471
Higuchi	0.9882	31.1304	2.2756
Korsmeyer-Peppas	0.9915 (Highest R^2)	24.3525 (Lowest MSC)	3.4052 (Highest AIC, Worst)

Table 7: Film evaluation parameters

Film	Film thickness	Film transparency	Weight variation	Folding endurance	Disintegration time	Surface pH	Drug content	Dissolution
Film 1	0.02± 0.01	Transparent	0.0218±0.0011	12.66±2.51	14±1	6.44±0.02	97.53±0.41	95.6900±0.8627
Film 2	0.04± 0.005	Transparent	0.0455±0.0027	16.66±2.08	14±1	6.55±0.03	97.03±0.47	92.9500±1.1879
Film 3	0.07±0.01	Transparent	0.0410±0.0004	18.33±3.51	17±1.52	6.60±0.03	98.53±0.64	96.0550±0.2192
Film 4	0.07±0.01	Transparent	0.0281±0.0022	30.66±3.05	11±1	6.83±0.04	94.25±0.08	95.8400±1.1314
Film 5	0.05±0.01	Transparent	0.0233±0.0025	6.0±2	16±1.73	6.74±0.02	95.50±0.30	92.5550±1.6193
Film 6	0.05±0.05	Transparent	0.0258±0.0019	27±3	13±3	6.71±0.02	96.60±0.36	95.9300±0.5233
Film 7	0.06±0.02	Transparent	0.0414±0.0031	8.0±3	19±1	6.85±0.03	96.40±0.36	91.9550±2.6092
Film 8	0.15±0.03	Transparent	0.0422±0.0019	3.0±1	22±1.73	6.71±0.03	94.30±0.40	91.2450±2.3405
Film 9	0.08±0.01	Transparent	0.0455±0.0037	51.33±4.04	09±1	6.45±0.03	96.36±0.51	97.7900±0.5515

Data is given in mean±SD (n=3)

Stability study of the OFDF

The stability study was performed as per ICH guideline Q1A (R2). The prepared formulation was wrapped uniquely. No change has been observed in the color. The parameters, like drug content, dissolution, and disintegration time, were evaluated after the completion of each month. The stability study values are provided in table 8.

Table 8: Stability study of the film

S. No.	Months	Drug content %	Dissolution %	Disintegration time sec
1.	Initial	98.53±0.64	96.21±1.79	17±2
2.	After1month	98.24±0.18	96.15±0.89	15±1
3.	After2months	97.96±0.72	97.24±2.78	16±3
4.	After3months	97.48±0.56	96.48±1.34	18±1

*Data is given in mean±SD. (n=3)

CONCLUSION

This study presents a process for extracting and preparing a nicotine-containing OFDF. This formulation allows smokers to receive a unit dose of nicotine as needed, helping to reduce withdrawal symptoms associated with tobacco or cigarette cessation. The film is particularly beneficial for older individuals who may find it challenging to use nicotine gums or e-cigarettes. When the extracted nicotine is incorporated into the oral film, it is rapidly released, stimulating the CNS and alleviating withdrawal symptoms. This technique is simple, cost-effective, and efficient. The resulting film disintegrates quickly and dissolves rapidly. *In vitro* drug release studies have shown promising results. Further, *in vivo* studies are essential in assessing the formulation's pharmacokinetics and bioavailability. Long-term stability studies will provide insights into product robustness. Additionally, future research can focus on clinical translation to improve patient compliance, ensure safety, and meet regulatory requirements for potential commercialization.

AUTHORS CONTRIBUTIONS

Investigation (S. D. P, T. M. K); resources (Y. B., L. L.); visualization (N. S.) writing – original draft (S. D. P.) writing – review and editing (all); supervision/validation (S. D. P, T. M. K., N. S., G. R.) conceptualization/methodology/funding acquisition/project administration (S. D. P, T. M. K., N. S.).

CONFLICTS OF INTERESTS

There are no conflicts to declare

REFERENCES

1. Feng K, Liu C, Zhang S, WU J, Eleuteri AM, Bai Y. Insights into the formation of pullulan nanofilm and its feasibility as probiotic resided oral fast-dissolving carrier. Int J Biol Macromol. 2025 Apr;299:140091. doi: 10.1016/j.ijbiomac.2025.140091, PMID 39842598.

2. LI Y, Zhao M, Zhao MY, LI B, Tian JL. Advances in oral dissolving film research in the food field. Food Prod Process Nutr. 2025;7(1):1-15. doi: 10.1186/S43014-024-00285-X.

3. Borges JG, DE Carvalho RA. Orally disintegrating films containing propolis: properties and release profile. J Pharm Sci. 2015 Apr.;104(4):1431-9. doi: 10.1002/JPS.24355, PMID 25631489.

4. Castro PM, Fonte P, Sousa F, Madureira AR, Sarmento B, Pintado ME. Oral films as breakthrough tools for oral delivery of proteins/peptides. J Control Release. 2015 Aug;211:63-73. doi: 10.1016/j.jconrel.2015.05.258, PMID 25979328.

5. View of formulation development of oral fast-dissolving films of rupatadine fumarate. Available from: https://journals.innovareacademics.in/index.php/ajpcr/article/view/39185/23832. [Last accessed on 10 Mar 2025].

6. Sevinc Ozakar R, Ozakar E. Current overview of oral thin films. Turk J Pharm Sci. 2021;18(1):111-21. doi: 10.4274/tjps.galenos.2020.76390, PMID 33634686.

7. Duren M, Atella L, Welding K, Kennedy RD. Nicotine pouches: a summary of regulatory approaches across 67 countries. Tob Control. 2023 Feb 7;tc-2022-057734. doi: 10.1136/tc-2022-057734, PMID 36750358.

8. Kasza KA, Tang Z, Seo YS, Benson AF, Creamer MR, ED wards KC. Divergence in cigarette discontinuation rates by use of electronic nicotine delivery systems (ENDS): longitudinal findings from the United States PATH study waves 1-6. Nicotine Tob Res. 2025 Jan;27(2):236-43. doi: 10.1093/NTR/NTAE027, PMID 38566367.

9. XU LL, Shi LL, Cao QR, Xu WJ, Cao Y, Zhu XY. Formulation and *in vitro* characterization of novel sildenafil citrate loaded polyvinyl alcohol polyethylene glycol graft copolymer based orally dissolving films. Int J Pharm. 2014 Oct;473(1-2):398-406. doi: 10.1016/j.ijpharm.2014.07.037, PMID 25079431.

10. Nishigaki M, Kawahara K, Nawa M, Futamura M, Nishimura M, Matsuura K. Development of fast dissolving oral film containing dexamethasone as an antiemetic medication: clinical usefulness. Int J Pharm. 2012 Mar;424(1-2):12-7. doi: 10.1016/j.ijpharm.2011.12.057, PMID 22240389.

11. Elkanayati RM, Darwesh AY, Taha I, Wang H, Uttreja P, Vemula SK. Quality by design approach for fabrication of extended release buccal films for xerostomia employing hot melt extrusion technology. Eur J Pharm Biopharm. 2024 Jul;200:114335. doi: 10.1016/j.ejpb.2024.114335, PMID 38768765.

12. Shah B, Khunt D, Bhatt H, Misra M, Padh H. Application of quality by design approach for intranasal delivery of rivastigmine loaded solid lipid nanoparticles: effect on formulation and characterization parameters. Eur J Pharm Sci. 2015 Oct;78:54-66. doi: 10.1016/j.ejps.2015.07.002, PMID 26143262.

13. Shaikh MV, Kala M, Nivsarkar M. Formulation and optimization of doxorubicin loaded polymeric nanoparticles using box-behnken design: ex-vivo stability and *in vitro* activity. Eur J Pharm Sci. 2017 Mar;100:262-72. doi: 10.1016/j.ejps.2017.01.026, PMID 28126560.

14. Camacho Vieira C, Peltonen L, Karttunen AP, Ribeiro AJ. Is it advantageous to use quality by design (QBD) to develop nanoparticle-based dosage forms for parenteral drug administration? Int J Pharm. May 2024;657:124163. doi: 10.1016/j.ijpharm.2024.124163, PMID 38670473.

15. Chakraborty A, Gupta A, Singh AK, Patni P. Effect of oxidative phytochemicals on nicotine-stressed UMNSAH/DF-1 cell line. J Tradit Complement Med. 2014 Apr;4(2):126-31. doi: 10.4103/2225-4110.126172, PMID 24860736.

16. Cosci F, Pistelli F, Lazzarini N, Carrozzi L. Nicotine dependence and psychological distress: outcomes and clinical implications in smoking cessation. Psychol Res Behav Manag. 2011;4:119-28. doi: 10.2147/PRBM.S14243, PMID 22114542.

17. Cahill K, Stead LF, Lancaster T. Nicotine receptor partial agonists for smoking cessation. Cochrane Database Syst Rev. 2008;3:CD006103. doi: 10.1002/14651858.

18. Pennington E, Bell S, Hill JE. Should video laryngoscopy or direct laryngoscopy be used for adults undergoing endotracheal intubation in the pre-hospital setting? A critical appraisal of a systematic review. J Paramed Pract. 2023;15(6):255-9. doi: 10.1002/14651858, PMID 38812899.

19. Nakajima M, Al Absi M. Nicotine withdrawal and stress-induced changes in pain sensitivity: a cross-sectional investigation between abstinent smokers and nonsmokers. Psychophysiology. 2014;51(10):1015-22. doi: 10.1111/PSYP.12241, PMID 24934193.

20. Breslau N, Kilbey MM, Andreski P. Nicotine dependence major depression and anxiety in young adults. Arch Gen Psychiatry. 1991;48(12):1069-74. doi: 10.1001/ARCHPSYC.1991.01810360033005, PMID 1845224.

21. Covey LS. Tobacco cessation among patients with depression. Prim Care. 1999 Sep;26(3):691-706. doi: 10.1016/S0095-4543(05)70124-X, PMID 10436294.

22. IM, CP, NA, BS, RJ, C Youths. Bonnie. In: Lynch. The nature of nicotine addiction; 1994. Available from: https://www.ncbi.nlm.nih.gov/books/NBK236759. [Last accessed on 13 Jan 2025].

23. Shamsudeen S, Kakunje A. Comments on: comparative evaluation of the efficacy of nicotine chewing gum and nicotine patches as nicotine replacement therapy using salivary cotinine levels as a biochemical validation measure. Indian J Psychiatry. 2024 Mar;66(1):119-20. doi: 10.4103/indianjpsychiatry.Indianjpsychiatry_631_23, PMID 38419920.

24. Mallock N, Schulz T, Malke S, Dreiack N, Laux P, Luch A. Levels of nicotine and tobacco-specific nitrosamines in oral nicotine pouches. Tob Control. 2024 Mar.;33(2):193-9. doi: 10.1136/TC-2022-057280, PMID 38378209.

25. Nicotine replacement therapy to help you quit tobacco. American Cancer Society. Available from: https://www.cancer.org/cancer/risk-prevention/tobacco/guide-quittingsmoking/nicotine-replacement-therapy.html. [Last accessed on 26 Mar 2025].

26. Wang Z, LI J, Yang H, SU X, Bushra R, Guo J. Optimized steam explosion treatment of tobacco stems for enhanced extraction of solanesol and nicotine. Ind Crops Prod. 2025 Mar;225:120470. doi: 10.1016/j.indcrop.2025.120470.

27. Agrupis S, Maekawa E, Suzuki K. Industrial utilization of tobacco stalks II: preparation and characterization of tobacco pulp by steam explosion pulping. J Wood Sci. 2000;46(3):222-9. doi: 10.1007/BF00776453.

28. Clayton PM, Vas CA, Bui TT, Drake AF, MC Adam K. Spectroscopic studies on nicotine and nornicotine in the UV region. Chirality. 2013 May;25(5):288-93. doi: 10.1002/CHIR.22141, PMID 23494810.

29. Sukweenadhi J, Tranku C, Ayu D, Kang SC. Optimizing nicotine extraction and analysis method from tobacco agrowaste extract. BIO Web Conf. 2024;104:00022. doi: 10.1051/bioconf/202410400022.

30. Fathi RM, Fauzantoro A, Rahman SF, Gozan M. Column chromatography isolation of nicotine from tobacco leaf extract (Nicotiana tabaccum L.). AIP Conf Proc. 2018;1927:030020. doi: 10.1063/1.5023958.

31. Barlow RB, Hamilton JT. The stereospecificity of nicotine. Br J Pharmacol Chemother. 1965;25(1):206-12. doi: 10.1111/j.1476-5381.1965.tb01773.x, PMID 19108199.

32. Yildiz D, Nicotine. Its metabolism and an overview of its biological effects. Toxicon. 2004 May;43(6):619-32. doi: 10.1016/j.toxicon.2004.01.017, PMID 15109883.

33. Clayton PM, Vas CA, Bui TT, Drake AF, MC Adam K. Spectroscopic studies on nicotine and nornicotine in the UV region. Chirality. 2013 May;25(5):288-93. doi: 10.1002/CHIR.22141, PMID 23494810.

34. Joseph A, Kumar GJ, Pawar SD, Hirlekar BU, Bharatam PV, Konda S. Analytical developments of p-hydroxy prenylamine reference material for dope control research: characterization and purity assessment. Drug Test Anal. 2022;14(2):224-32. doi: 10.1002/dta.3171, PMID 34617411.

35. Al Dahhan WH, Kadhom M, Yousif E, Mohammed SA, Alkaim A. Extraction and determination of nicotine in tobacco from selected local cigarettes brands in Iraq. Lett Appl Nano Bio Sci. 2021;11(1):3278-90. doi: 10.33263/LIANBS111.32783290.

36. Ning Y, Zhang LY, Mai J, SU JE, Cai JY, Chen Y. Tobacco microbial screening and application in improving the quality of tobacco in different physical states. Bioresour Bioprocess. 2023 Dec;10(1):32. doi: 10.1186/S40643-023-00651-6, PMID 38647749.

37. Pawar SD, Gawali K, Kulhari H, Murty US, Kumar P. Amoxapine loaded solid lipid nanoparticles with superior preclinical pharmacokinetics for better brain delivery: LC-MS/MS and GC-MS analysis. ACS Chem Neurosci. 2023;14(8):1388-98. doi: 10.1021/acschemneuro.2c00673, PMID 37027804.

38. Yang J, Liu ZH, Zhu RZ, Xiang NJ, Tang SY, HE P. X-ray powder diffraction data for nicotine 3,5-dihydroxybenzoate dihydrate, C10H15N2·C7H5O4·2H2O. Powder Diffr. 2021 Mar;36(1):25-8. doi: 10.1017/S0885715621000014.

39. Pawar SD, Gawali K, Jat S, Singh P, Datusalia AK, Kulhari H. Physiochemical characterization and pharmacokinetic assessment of bergamottin solid lipid nanoparticles. J Drug Deliv

40. Singh C, Rao K, Yadav N, Bansal N, Vashist Y, Kumari S. A review: drug excipient incompatibility by ftir spectroscopy. Curr Pharm Anal. 2023 Feb;19(5):371-8. doi: 10.2174/1573412919666230228102158.

41. Suryawanshi D, Wavhule P, Shinde U, Kamble M, Amin P. Development optimization and *in vivo* evaluation of cyanocobalamin loaded orodispersible films using hot melt extrusion technology: a quality by design (QbD) approach. J Drug Deliv Sci Technol. 2021 Jun;63:102559. doi: 10.1016/j.jddst.2021.102559.

42. The place of drug product critical quality parameters in quality by design (QBD). Available from: https://www.researchgate.net/publication/281925128_The_place_of_drug_product_critical_quality_parameters_in_quality_by_design_QBD. [Last accessed on 01 Feb 2025].

43. Sanchez MF, Luciani Giacobbe LC, Barbieri F, Olivera ME. Defining critical quality attributes and composition parameters for burn wound dressings: antibiotic anesthetic films as a model. Heliyon. 2024 Nov;10(22):e39766. doi: 10.1016/j.heliyon.2024.e39766, PMID 39605837.

44. Bharti K, Mittal P, Mishra B. Formulation and characterization of fast dissolving oral films containing buspirone hydrochloride nanoparticles using design of experiment. J Drug Deliv Sci Technol. 2019 Feb;49:420-32. doi: 10.1016/j.jddst.2018.12.013.

45. Priyanka, Kumar K, Teotia D. A comprehensive review on pharmaceutical oral dissolving films. J Drug Delivery Ther. 2019;9(5):170-4. doi: 10.22270/jddt.v9i5-s.3641.

46. Joshi P, Patel H, Patel V, Panchal R. Formulation development and evaluation of mouth dissolving film of domperidone. J Pharm Bioallied Sci. 2012 Mar;4 Suppl 1:S108-9. doi: 10.4103/0975-7406.94159, PMID 23066181.

47. International conference on harmonisation of technical requirements for registration of pharmaceuticals for human use ICH harmonised tripartite guideline stability testing of new drug substances and products Q1A(R2); 2003.

48. Taufik M, Ardilla D, Razali M, Susilawati E, Afniwati, Fadillah N. Extraction and analysis of nicotine from the saliva of active smokers using UV spectroscopy. In: proceedings of the 1st international mipanet conference on science and mathematics. Scitepress Science and Technology Publications; 2019. p. 616-20. doi: 10.5220/0010614700002775.

49. Mihranyan A, Andersson SB, EK R. Sorption of nicotine to cellulose powders. Eur J Pharm Sci. 2004 Jul;22(4):279-86. doi: 10.1016/j.ejps.2004.03.012, PMID 15196584.

50. Wang H, George G, Bartlett S, Gao C, Islam N. Nicotine hydrogen tartrate loaded chitosan nanoparticles: formulation characterization and *in vitro* delivery from dry powder inhaler formulation. Eur J Pharm Biopharm. 2017 Apr;113:118-31. doi: 10.1016/j.ejpb.2016.12.023, PMID 28088005.

51. LI ZQ, Shang SZ, Liao XX, Lei P, Han JM, YI B. X-ray powder diffraction data for nicotine 2,6-dihydroxybenzoate, C10H15N2·C7H5O4. Powder Diffr. 2022;37(2):105-7. doi: 10.1017/S0885715622000070.

52. Alaei S, Omidi Y, Omidian H. *In vitro* evaluation of adhesion and mechanical properties of oral thin films. Eur J Pharm Sci. 2021 Nov;166:105965. doi: 10.1016/j.ejps.2021.105965, PMID 34375679.

53. Dinge A, Nagarsenker M. Formulation and evaluation of fast dissolving films for delivery of triclosan to the oral cavity. AAPS Pharm Sci Tech. 2008 Jun;9(2):349-56. doi: 10.1208/s12249-008-9047-7, PMID 18431674.